IOPscience

Classical molecular dynamics simulations of amorphous silica surfaces

Classical molecular dynamics simulations of amorphous silica surfaces

M Rarivomanantsoa, P Jund and R Jullien

Laboratoire des Verres—Université Montpellier 2, Place E Bataillon Case 069,
34095 Montpellier, France

Abstract

We have adapted classical molecular dynamics to study the structural and dynamical properties of amorphous silica surfaces. Concerning the structure, the density profile exhibits oscillations perpendicularly to the surface as observed in liquid metal surfaces and the pair correlation functions as well as the angle distributions show features (absent in the interior of the films) that can be attributed to the presence of twofold rings which are perpendicular to the surface. From the mean-squared displacement of the non-bridging oxygen atoms we find that in the interior region they move perpendicular to the surface while they move parallel to it in the surface region.

1. Introduction

Most studies on surfaces have been focused on their electronic aspect. The goal was usually to analyse materials used in electronic devices of which the characteristics depend on the surface properties. As a consequence, crystalline surfaces are currently well known and a lot of attention has been devoted to the doping and transport properties of these surfaces as well as to the surface reconstruction. In recent years, many studies, theoretical [1] or experimental [2] have also been devoted to the analysis of liquid metal surfaces. In particular, the existence of an atomic layering in the density profile has been found. A great interest in understanding amorphous surfaces exists [3], because of their participation in the glass formation, and therefore several numerical studies are now available on this subject [4–6]. Pioneering work in using classical potentials to describe amorphous silica surfaces is due to Garofalini *et al*, who studied mainly the presence of defects (non-bridging oxygens (NBOs), small-sized rings. . .) at the surface [4]. These defect sites are the most chemically reactive ones but experimental studies have, so far, not clearly shown their existence [3, 7]. An alternative way to learn more about the surface is to study the chemical reactions taking place on it [8] and in particular the interaction between water and amorphous SiO_2 surfaces has been the topic of both experimental [9, 10] and numerical studies [11, 12]. In most of the numerical studies available in the literature, the total number of atoms did not exceed 800 and only a fraction

of these atoms were considered as 'mobile' (i.e. participating in the formation of the surface). (It should be noted that very recently (in fact during the process of writing the present article) a molecular-dynamics study of silica surfaces has been proposed involving several thousands of atoms [6]). Moreover the long-range Coulomb forces were either cut off [4] or treated in a *pseudo*-2D geometry [13], not taking into account exactly the reduced dimensionality of free silica surfaces. A recent study of the influence of long-range forces on the structure and dynamics of a model silica glass has shown that over-damped Coulomb interactions can alter the quality of the results [14].

In the present work the molecular dynamics force calculation scheme has been adapted to the specific 2D geometry of samples with free surfaces. Our aim was mainly to study in detail the structural properties of amorphous silica surfaces with respect to what is already known for the corresponding bulk samples and to test the quality of the widely used 'BKS' potential proposed by van Beest *et al* [15]. This classical pair potential describes quite well the structural [16, 17], and vibrational [18], as well as relaxational [19] and thermal [20] properties of both supercooled viscous liquid and glassy bulk silica samples: it is therefore justified to address its effectiveness in the case of 'bi-dimensional' silica systems, even more so since in a recent study based on *ab initio* simulations, Ceresoli *et al* have put into question the structural description of the surfaces obtained with the BKS potential [21]. In addition to the work already proposed by Roder *et al* [6], who used the same potential but aimed their study mainly at silica *clusters*, we show that the effect of the surface is firstly reflected in the density profile, which exhibits stratification, explained as a tendency to have more short range order at the surface. We then analyse in detail the ring size distribution as well as the orientation of the rings with respect to the surface, and show that the number of twofold rings (whose signature is visible in the radial pair distribution functions and the angle distributions) is coherent with the experimental estimates and that they are positioned perpendicularly to the surface. By analysing the influence of the annealing time on this effect, we show that it is a true surface reconstruction and not an artifact due to out-of equilibrium phenomena. Finally, in order to elucidate the diffusion process at the surface, we present the mean square displacement of the bridging and non-bridging oxygen atoms. We find no signature of a liquid-like behaviour at the surface but the dynamics of the NBOs seems to be anisotropic.

2. Simulations

We have performed classical molecular dynamics simulations starting with cubic samples of edge length $L = 35.80$ Å, containing 3000 particles. These samples were used previously to study the properties of bulk silica, therefore their mass density is $\rho \simeq 2.18$ g cm^{-3}, which is very close to the experimental value of 2.20 g cm^{-3} [22], and the periodic boundary conditions were assumed in the three space directions. The potential used to describe the interactions between the atoms is the two-body 'BKS' potential. After the use of this potential to study densified silica samples [23], we apply it here to study silica surfaces assuming this potential is still valid in the case of SiO$_2$ free surfaces. Of course this description can never be as accurate as an *ab initio* study; nevertheless we can simulate much larger samples and typical structural features should not depend on the details of the potential. The classical equations of motion are resolved by using the velocity-Verlet algorithm with a timestep $\Delta t = 0.7$ fs. The initial configuration is given by a bulk sample of amorphous silica at $T = 0$ K. This configuration has been obtained by quenching a well equilibrated liquid sample around 7000 K with a quench rate of 2.3×10^{14} K s^{-1}. The free surfaces are created by breaking the periodic boundary conditions along the z-direction, normal to the surface, thus creating two free surfaces located at $L/2$ and $-L/2$. Doing so, the Ewald summation for the calculation of the long range forces has to be

modified to take into account the loss of periodicity in the z-direction. There exists no standard method since several possibilities based on either a modified Ewald summation [13, 24] or multipole expansions [25] are proposed in the literature. A purely two-dimensional method exists [26], which nevertheless necessitates the adjunction of charged plates. Here we have chosen a strictly two-dimensional *approximate* technique, which has the advantage of being very simple [27]. In the three-dimensional Ewald summation technique, one considers all the point charges surrounded by a spherical distribution of charges that has the same magnitude but opposite sign [28]. Then, the potential is separated into two terms. The first term V_c corresponds to the potential due to the point charge distribution minus that of the screening spherical charge distribution and is quite rapidly convergent in real space. The second one V_γ is the potential created by the spherical distribution and is rapidly convergent in the reciprocal space. Since the real space term is a short range potential with a spherical symmetry, there is no need to change it for the two-dimensional summation. But, of course the reciprocal space potential has to be modified. While for the 3D Ewald summation the expression for the reciprocal space term of the potential is

$$V_\gamma = \frac{2\pi}{L^3} \sum_{\vec{k} \neq 0} \frac{1}{k^2} e^{-\frac{k^2}{4\kappa^2}} \left| \sum_i q_i e^{-i\vec{k}\vec{r_i}} \right|^2 \tag{1}$$

with

$$\vec{k} = n_x \frac{2\pi}{L} \vec{e_x} + n_y \frac{2\pi}{L} \vec{e_y} + n_z \frac{2\pi}{L} \vec{e_z}. \tag{2}$$

In our approximate two-dimensional method it becomes

$$V_\gamma = \frac{\pi}{L^2} \sum_{\vec{k} \neq 0} \frac{e^{-\frac{k^2}{4\kappa^2}}}{k} \left| \sum_i q_i e^{-i\vec{k}\vec{r_i}} \right|^2 \tag{3}$$

with

$$\vec{k} = n_x \frac{2\pi}{L} \vec{e_x} + n_y \frac{2\pi}{L} \vec{e_y}. \tag{4}$$

Here $\vec{k}$ is a two-dimensional vector and the summation runs over the two integers n_x and n_y. Although formula (3) looks like a straightforward two-dimensional transcription of formula (1) it is only approximate. The expression would have been exact if, instead of a Coulomb potential with a spherical symmetry, one had considered a cylindrical potential. In particular, one practical consequence is that the k-contribution to the z-component of the force is zero, since the scalar product $\vec{k}\vec{r_i}$ is independent of the third coordinate z_i of $\vec{r_i}$. We have used the characteristic constant $\kappa = 5.0/L$, where L is the cubic box size, and considered 49 k-vectors in reciprocal space to insure a relative error smaller than 2×10^{-5} for the potential energy. The removal of the periodic boundary conditions in the z-direction breaks the bonds between the atoms at the 'bottom' and those at the 'top' of the film. This will lead to bond rearrangements near each free surface and of course increase the temperature of the system. It is also worth noticing that we let the position of the atoms adjust freely in the z-direction and therefore we are not *stricto sensu* in a microcanonical ensemble. To justify *a posteriori* the approximations and check the results we compared this method with the one in which the box length in the z-direction, L_z, is artificially increased in order to simulate a pseudo-2D system. We find that the two techniques give similar results when L_z is five times larger than the box length in the other two directions, which is in contrast with the study of Bakaev *et al* [12], in which L_z was taken only twice as large as in the x and y directions. In any case the method used here is computationally much more efficient since the number of k-points included in the Ewald

summation has not to be increased. It is also faster than the more frequently used technique proposed in [13], which is not a strictly 2D technique and which is computationally very costly.

The heating of the slab mentioned earlier will tend to evaporate some oxygen atoms located at the surface, and to avoid this vaporization, it is necessary to control the temperature of the slab. This has been done at 1000 K by rescaling the velocities during 30 000 time steps. This temperature is below the simulated glass transition temperature as will be shown in a forthcoming study. Then the system was allowed to relax 30 000 supplemental steps and finally we performed simulations during 60 000 supplemental steps to collect the results, the system temperature remaining almost constant around 1000 K in this time range. Such a simulation represents 45 days of computer time on the latest IBM-SP2 processor and in order to improve the statistics of the data we averaged our results over ten independent liquid samples.

3. Results

In figure 1 we have reported the averaged density profile of our samples in the z-direction. Each point (filled circle) of the figure corresponds to the density $\rho(z)$ calculated within a slab
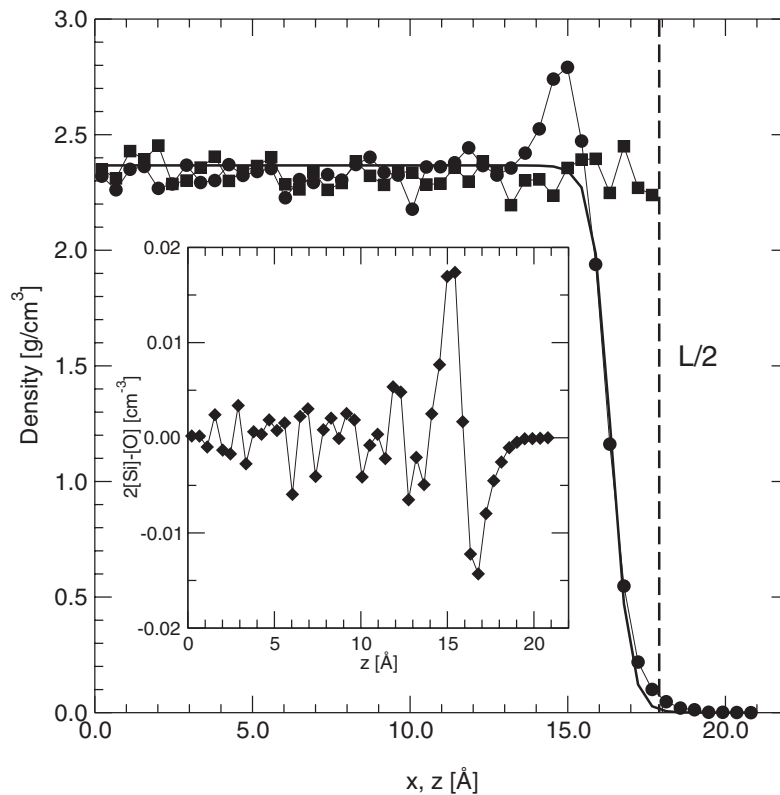

Figure 1. Density profile $\rho(z)$ in the direction z, perpendicular to the surface, from $z = 0$ (median cut of the simulation box) up to the outer part of the surface. The filled circles correspond to the density calculated within slabs of width $\Delta z = 0.4475$ Å for a sample size of $L = 35.8$ Å. The densities for slabs of opposite coordinates z have been averaged. The curve represents the fit of $\rho(z)$ using equation (5). In the inset the quantity $\Delta n = 2[Si] - [O]$ is plotted as a function of z, where $[Si]$ and $[O]$ are the numbers of Si and O atoms per unit volume calculated within the slabs.

parallel to the surface of area $L \times L$ and of width $\Delta z = 0.4475$ Å and reported as a function of the mean slab position z. We have averaged the results over the two slabs located at z and $-z$. For comparison, we have reported the profile in the x-direction calculated within a slab of the same width $\Delta x = 0.4475$ Å but of area $L \times L_z$ with $L_z = 26.85$ Å, taken sufficiently smaller than L to avoid edge effects due to the presence of the free surface in the z-direction. In both cases, we get an average bulk density of about 2.3 g cm^{-3}, significantly larger than the density $\rho = 2.18$ g cm^{-3} of the original cubic box with periodic boundary conditions. This increase of the density is due to the relaxation of the system (the system contracts along the z-direction) when creating the free surfaces since it has been shown that the equilibrium density of the BKS potential is larger than the experimental one [29] (this means that the initial sample with PBC had a negative pressure). This shows that creating free surfaces is a physical way to obtain the equilibrium density and thus permits us also to validate *a posteriori* our *modus operandi*. For the profile in the z-direction, one can use a hyperbolic tangent fit derived from the Van der Waals theory of surface tension [30]. Although this formula is generally used to study the thermodynamic properties of simple liquids, some characteristics of the density profile of our amorphous samples can be determined. This fit uses three parameters, ρ_0, the mass density in the underlying bulk, z_0, the position of the surface, and d, the surface thickness:

$$\rho(z) = \frac{\rho_0}{2}\left(1 - \tanh\left(\frac{2(z - z_0)}{d}\right)\right). \tag{5}$$

In fact, this formula fits very well the vapour–liquid interfaces which exhibit symmetric density profiles [30]. But here it does not take into account the asymmetric density maximum near the free surfaces (see figure 1) and therefore the density profile is not very well fitted near this maximum. As a consequence, if the parameter ρ_0 ($\rho_0 = 2.36$ g cm^{-3}) gives a good quantitative value for the bulk density, the parameter d ($d = 1.18$ Å) gives only a rough (underestimated) value of the actual surface thickness. As observed for liquid surfaces [31], we have an asymmetric peak with a broad tail in the density profile at the surface and a layering behaviour. Our goal is to identify the participation of the stratification in the oscillations observed in the density profile along the z-direction. However when comparing the density profiles in the z- and x-directions in figure 1, one can hardly see a difference in the oscillations around the plateau. One way to address this point is to compute the standard deviation of these data over different samples. If the oscillations are only due to statistical fluctuations, the standard deviation σ of the density should behave like $N_S^{-1/2}$, where N_S is the number of statistical independent samples over which the density profiles are averaged. Along the x- and y-axes, we find that the standard deviations behave like $N_S^{-1/2}$ while for the z-direction they are quite independent of N_S. Therefore the oscillations along the z-direction are most likely a signature of a layer formation whereas the oscillations observed in the x-direction are only due to statistical density fluctuations. This stratification is likely to be enhanced at the free surfaces and to extend in the underlying bulk. Computing the radial pair distribution for atoms within a sphere of radius $R = L/4$, whose centre is the centre of the initial cubic box, we found that it is similar to that observed for bulk amorphous silica samples. This is an evidence that the layering behaviour is not due to crystallization. The inset of figure 1 exhibits the contribution of each type of atom to the mass density. Since the stoichiometry is respected, the quantity $\Delta n = 2[\text{Si}] - [\text{O}]$ is oscillating around a zero mean within the underlying bulk. Near the surface, the apparition of two peaks reflects some stoichiometry breaking. The silicon atom excess under the surface and the oxygen atom excess at the surface are respectively represented by the positive and the negative peak. This surface segregation appears not to be model dependent since it has been found also by Roder *et al* [6] as well as by Litton and Garofalini [32] with another potential.
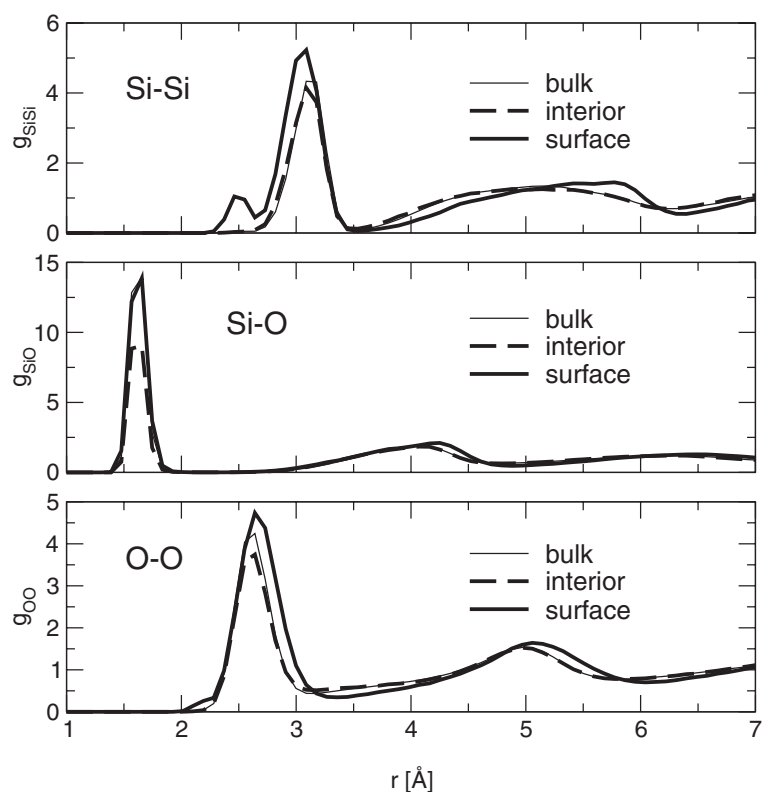
Figure 2. Radial pair distribution functions in a bulk silica sample (thin solid), in the interior region of our silica film (dashed) and in the surface region (solid bold) (see the text for the definition of the regions).

In figure 2 we present the radial pair distribution functions (RPDFs) for the different pairs of atoms in order to investigate the structure of our samples. The space has been divided into two regions, the 'surface' layer, which extends 6 Å below the z-position of the outermost atom, and the 'interior', which represents the rest of the sample. The width of the surface layer has been chosen to encompass the broad peak in the density profile visible in figure 1 and is coherent with previous studies [6]. Also shown in figure 2 are the RPDFs obtained in a bulk silica sample. As a general trend, the RPDFs in the interior are very similar to the ones obtained in the bulk. Nevertheless differences can be seen especially in the O–O RPDF, where a slight shift towards smaller distances can be seen. This is a consequence of the relaxation towards a higher equilibrium density. The major difference between the surface and the interior can be seen in the Si–Si RPDF, since a small shoulder appears around 2.5 Å. This shoulder, which can be attributed to two-membered rings as we will see below, is absent in the interior or bulk curve since this structural unit is not present in the bulk [14, 17, 33]. In figure 3 we show the distribution functions of the angle between an oxygen (silicon) atom and its two silicon (oxygen) neighbours (two atoms are neighbours if their separation is smaller than the location of the first minimum in the corresponding RPDF) where we distinguish again the surface, the interior and the results obtained for bulk silica (this is a further test of the validity of the BKS potential, which does not contain three-body terms). Concerning the O–Si–O angle distribution, there is almost no difference between the interior and the bulk. The distribution at
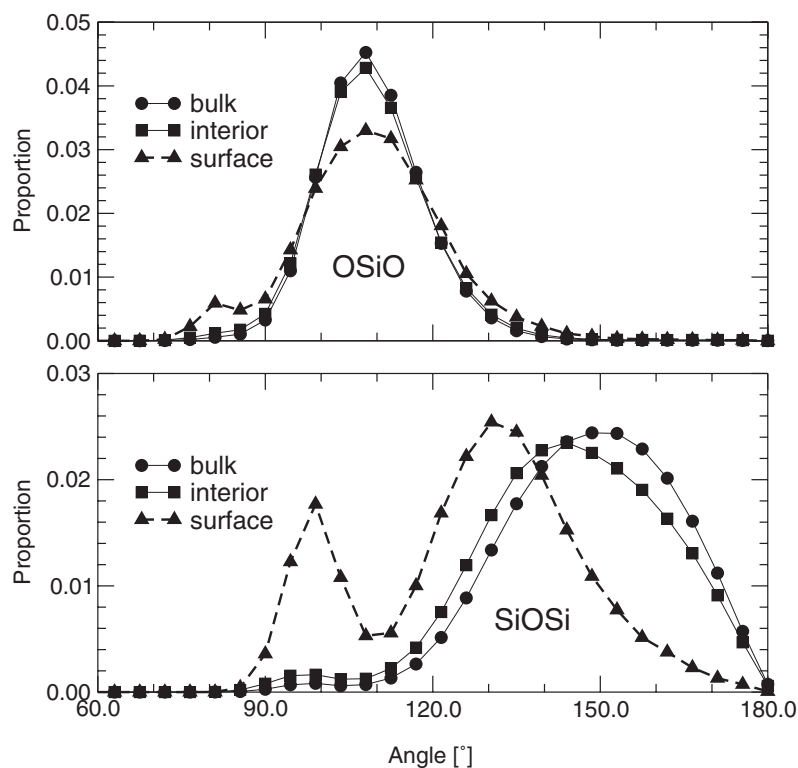
Figure 3. O–Si–O and Si–O–Si angle distributions in a bulk silica sample (circles), the interior (squares) and surface (triangles) regions of our silica film.

the surface is slightly broader and shows a second peak around 80° which is absent in the bulk. Concerning the Si–O–Si angle distribution we firstly note a slight shift of the whole distribution towards smaller angles compared to the bulk distribution, which is again a consequence of the density relaxation. Next we note a strong shift of the surface distribution towards smaller angles by more than 10°, which is coherent with the peak in the density profile observed in figure 1 and an important second peak around 100°, which is absent in the bulk and interior curves. The existence of the additional peaks in the surface angle distributions is in agreement with previous studies [4, 6]. The location of these peaks is different from the angles O–Si–O and Si–O–Si expected in two-membered rings [34]: 94 and 86° respectively. Here we find 80 and 100°, which indicates a weakness of the pair potential on this particular point since in a recent *ab initio* study on silica clusters Lopez *et al* found 91 and 89° respectively [37].

So far we only have the signature of the presence of two-membered rings at the surface, therefore it is justified to address the influence of the free surfaces on the variation of the ring size distribution. Such quantity is of interest since it can be extracted from infrared and Raman spectroscopy. In particular the highly strained two-membered rings result in infrared-active Si–O stretching modes at 888 and 908 cm^{-1} [35, 36]. The ring size distribution has been determined using the algorithm described in [19], where a ring is defined as the smallest loop starting from one oxygen atom O_1 nearest neighbour of a given Si atom and ending on O_2, another of its nearest neighbours. Then the size of a ring is given by the number of its constitutive Si–O segments. To get the distribution of each ring size along the z-axis in the
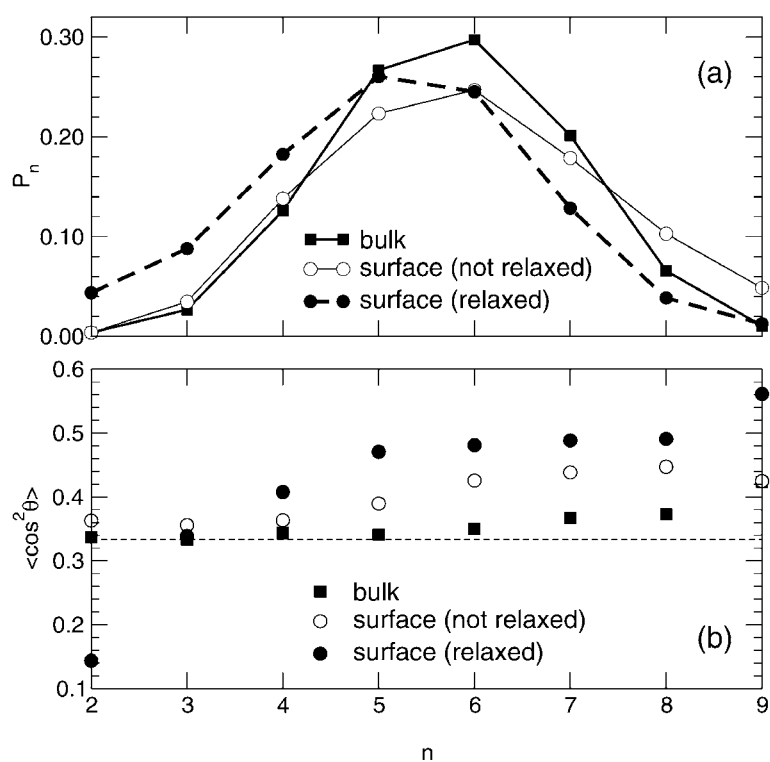
Figure 4. (a) Plot of P_n versus n in a bulk silica sample, in the initial surface region (not relaxed) and in a 42 ps annealed surface region (relaxed) where P_n is the probability that an atom in a given region is a member of an n-fold ring. (b) Plot of $\langle \cos^2 \theta \rangle$ as a function of the ring size n, where θ is the angle between the direction perpendicular to the surface and the direction perpendicular to the ring. The dashed line represents $\langle \cos^2 \theta \rangle = \frac{1}{3}$ corresponding to an isotropic orientation of the rings.

two regions (interior and surface) we compute the probability P_n for a given Si atom, whose coordinate along the normal direction to the surface is in a given region, to be a member of a n-fold ring. These results are reported in the top part of figure 4 and compared to the bulk distribution. We calculated the ring size distribution in the surface layer on the initial 2D samples (not relaxed) and on the 2D samples annealed for 42 ps (relaxed) in order to see the influence of the annealing time on the results. Firstly it should be noted that the distributions in the interior region (relaxed or not relaxed) are very similar to the bulk distribution (which is a broad Gaussian centred around sixfold rings [14]) and are therefore not reported in figure 4(a). The situation is different at the surfaces, where the global trend after the annealing period is a decrease of the probability for a Si atom to be a member of a large ring (as expected, since a lot of bonds are broken) together with an increase of the probability to be a member of a small ring, more precisely, twofold, threefold and fourfold rings. A particular case of this behaviour is the inversion of the proportion of fivefold and sixfold rings at the annealed surface. Energetically, there is no significant difference between these two ring sizes, therefore if sixfold rings are broken at the surface (because they are relatively large) a fraction of these rings will become fivefold and fivefold rings will become predominant: in a sense this corresponds to the reconstruction of an amorphous surface. Another significant feature is the relatively large proportion of twofold rings at the annealed surface whereas it stays very weak in the bulk and

at the freshly created surface. More precisely we find an average density of 0.25 rings nm^{-2}, which is in the range of the experimental values, which vary between 0.1 and 0.4 rings nm^{-2} [10, 34, 35]. This proportion is smaller than that found in [6] (0.6 rings nm^{-2}), where the statistics were done at 3000 K and for silica clusters at equilibrium (which is certainly not the case here).

Together with the ring size distribution we have also investigated the ring orientations by computing $\langle \cos^2 \theta \rangle$, for a given ring size n, within a given region of the sample, where θ is the angle between the normal to the surface and to the ring. The results for the surface region are reported at the bottom of figure 4 as a function of the annealing time, and compared with those obtained in a 3D sample (which are similar to those in the interior region). In the bulk, all the n-fold rings are oriented in an isotropic way since the value of $\langle \cos^2 \theta \rangle$ is close to one-third. In the freshly created surface region, the two-, three- and fourfold have still an isotropic orientation, while the larger rings are oriented rather parallel to the surface since $\langle \cos^2 \theta \rangle$ is slightly larger than one-third. In the annealed surface layer we note that the rings larger than the threefold ones have a strong tendency to orient parallel to the surface. In contrast the twofold rings are now perpendicular to the surface since $\langle \cos^2 \theta \rangle$ is much smaller than one-third. This is a result of the annealing and can therefore be extrapolated to a film in equilibrium in which twofold rings are certainly a oriented perpendicular to the surface. This is coherent with the *ab initio* study of Ceresoli *et al* [21], even if they had only one twofold ring at the surface.

After the description of the structure let us now turn in the final part of this work to the diffusion mechanism inside our thin silica films. The motivation of this study is connected to the idea that similarly to crystalline faces which develop a microscopic liquid film [38] the surface layers of an amorphous sample show an enhanced diffusivity compared to the bulk [32, 39]. The simplest way to address this question is to compute the mean-squared displacement (MSD) $\langle r^2(t) \rangle = \langle |r_i(t) - r_i(0)|^2 \rangle$ for a given particle type i. This is what is represented in figure 5 for the oxygen atoms (the behaviour of the silicon atoms is qualitatively similar as shown in [6]). The interior and surface regions have been determined with respect to the *initial* position of the atoms. In figure 5 we have also distinguished the behaviour of the non-bridging oxygens (NBOs) from that of the bridging oxygens (BOs). At the surface we find approximately 15% of NBOs while in the interior only 0.5% of the oxygen atoms are single coordinated, which is in good agreement with a recent MD study of nanoporous silica [40], especially for the number of NBOs in the surface region. We have also calculated the components of the MSD that are parallel ($1.5\langle x^2 + y^2 \rangle$) and perpendicular ($3\langle z^2 \rangle$) to the surface, and these components are also represented in figure 5. In order to study the influence of the annealing time, the MSD has been calculated for 42 ps at the beginning of the relaxation process (thin lines) and after an annealing time of 105 ps (bold lines). For the BOs there is no difference in the MSD between the interior and the surface region. After the annealing period, the displacement of the atoms is smaller and more isotropic. Hence for a fully equilibrated film the dynamics of the particles inside the sample is expected to be almost isotropic.

For the NBOs the situation is different. Firstly as expected, the NBOs diffuse more than the BOs. Next, after annealing, the dynamics appear to be more *anisotropic* in both regions (interior and surface). In the interior region the perpendicular MSD is more important than the parallel one as if the NBOs were attracted towards the surface. In contrast in the surface layer the NBOs move parallel to the surface rather than perpendicular to it. This can be understood since most of the Si–O bonds point outward from the surface and since it is easier for an NBO to have a bond 'bending' motion rather than a bond 'stretching' motion. Therefore concerning the NBOs, we find that their dynamics is anisotropic both in the interior and the surface region. Since this anisotropy is enhanced after annealing one can expect that this behaviour is also true in an equilibrated sample.
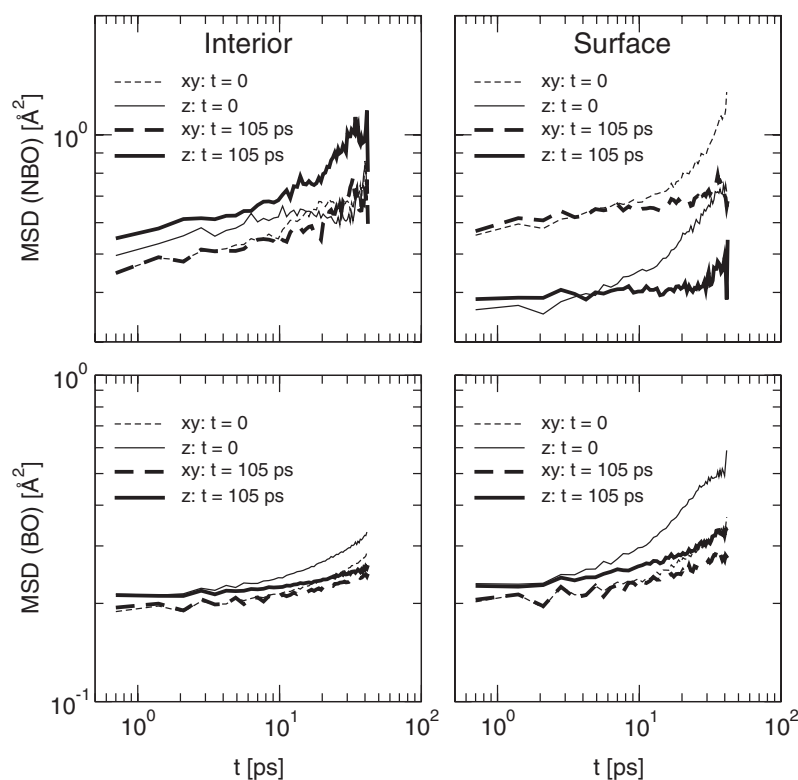
Figure 5. Plot of the mean squared displacement (MSD) of the bridging oxygens (BO) and non-bridging oxygens (NBO) in the interior and surface regions as a function of the annealing time. We have distinguished the parallel component of the MSD $1.5\langle x^2 + y^2\rangle$ (dashed and labelled xy) and the perpendicular component $3\langle z^2\rangle$ (solid and labelled z).

4. Conclusion

We have used classical molecular dynamics to study the structural properties and the mean squared displacement of the particles inside an amorphous silica film. The first step in this work was to adapt our computational method to samples without periodic conditions in one spatial direction. This has been done using an original method which is fast and relatively accurate. With this technique we have calculated the density profile along the normal direction z to the surface. We have found that the system is contracting since the equilibrium density of the potential is greater than the mass density of the initial amorphous silica sample. This relaxation is rather fast and creating a surface seems therefore to be a physical and efficient way to obtain the equilibrium density of a given system. This shows also that the BKS potential describes properly the physics inherent to the creation of free surfaces. As in liquid metals, the density profile exhibits a layering behaviour that seems to be enhanced at the surface. This feature was interpreted as a sign of an increase of the short range order near the surface. The asymmetric peak near the surface is a sign of a stoichiometry breaking: while the silicon atoms are in excess in the inner part of the surface the oxygen atoms are in excess in its outer part as already mentioned in previous studies [4, 6]. We have calculated also the radial pair distribution functions and the angle distributions and we found the signature of the presence of twofold rings at the surface similarly to previous studies [6]. Therefore we have also focused

our attention on the ring size distribution and ring orientation along the z-direction. We see that at the free surfaces, the most energetically unfavourable configurations (small rings) are enhanced and correlatively, the large rings show a tendency to disappear. A particular case of this feature is the inversion of the proportion of fivefold and sixfold rings. Also the orientation of the small-sized rings with respect to the surface (twofold rings are perpendicular to the surface) agrees well with a recent *ab initio* study [21]. Concerning the MSD of the oxygen atoms, we find that the dynamics of the BOs is unaffected by the presence of the surface. In contrast the dynamics of the NBOs is clearly anisotropic: in the interior (far from the surface) they move rather perpendicular to the surface while in the surface region they move parallel to it.

Acknowledgment

References

[1] Iarlori S, Carnevali P, Ercolessi F and Tosatti E 1989 *Europhys. Lett.* **10** 329
Iarlori S, Ercolessi F and Tosatti E 1991 *Surf. Sci.* **251/252** 951
Celestini F, Ercolessi F and Tosatti E 1997 *Surf. Sci.* **377–379** 914
[2] Magnussen O, Ocko B M, Regan M J, Penanen K, Pershan P S and Deutsch M 1995 *Phys. Rev. Lett.* **74** 4444
Regan M J, Kawamoto E H, Pershan P S, Maskil N, Deutsch M, Magnussen O M, Ocko B M and Berman L E 1995 *Phys. Rev. Lett.* **75** 2498
[3] See for example Pantano C G 1989 *Rev. Solid State Sci.* **3** 379
[4] Garofalini S H 1983 *J. Chem. Phys.* **78** 2069
Levine S M and Garofalini S H 1987 *J. Chem. Phys.* **86** 2997
Feuston B P and Garofalini S H 1989 *J. Chem. Phys.* **91** 564
[5] Kilian K A, Drabold D A and Adams J B 1993 *Phys. Rev.* B **48** 17 393
Dong J and Drabold D A 1998 *Phys. Rev.* B **57** 15 591
Branda M M, Montani R A and Castellani N J 2000 *Surf. Sci. Lett.* **446** 89
[6] Roder A, Kob W and Binder K 2001 *J. Chem. Phys.* **114** 7602
[7] Hochstrasser G and Antonini J F 1972 *Surf. Sci.* **32** 644
Sprenger D, Bach H, Meisel W and Gutlich P 1990 *J. Non-Cryst. Solids* **126** 111
[8] Morrow B A and McFarlan A J 1990 *J. Non-Cryst. Solids* **120** 61
[9] Krol D M and van Lierop J G 1984 *J. Non-Cryst. Solids* **68** 163
Kinney D R, Chuang I and Maciel G E 1993 *J. Am. Chem. Soc.* **115** 6786
[10] Grabbe A, Michalske A and Smith W L 1995 *J. Phys. Chem.* **99** 4648
[11] Feuston B P and Garofalini S H 1990 *J. Appl. Phys.* **68** 4830
Bogillo V I, Pirnach L S and Dabrowski A 1997 *Langmuir* **13** 928
[12] Bakaev V A and Steele W A 1999 *J. Chem. Phys.* **111** 9803
[13] Parry D E 1975 *Surf. Sci.* **49** 433
Parry D E 1976 *Surf. Sci.* **54** 195
Heyes D M 1984 *Phys. Rev.* B **30** 2182
Heyes D M 1994 *Phys. Rev.* B **49** 755
[14] Jund P, Rarivomanantsoa M and Jullien R 2000 *J. Phys.: Condens. Matter* **12** 8777
[15] van Beest B, Kramer G and van Santen R 1990 *Phys. Rev. Lett.* **64** 1955
[16] Jund P and Jullien R 1999 *Phil. Mag.* A **79** 223
[17] Vollmayr K, Kob W and Binder K 1996 *Phys. Rev.* B **54** 15 808
[18] Taraskin S N and Elliott S R 1997 *Europhys. Lett.* **39** 37
[19] Horbach J and Kob W 1999 *Phys. Rev.* B **60** 3169
[20] Jund P and Jullien R 1999 *Phys. Rev.* B **59** 13 707
[21] Ceresoli D, Bernasconi M, Iarlori S, Parinello M and Tosatti E 2000 *Phys. Rev. Lett.* **84** 3887
[22] Mazurin O V, Streltsina M V and Shvaiko-Shvaikovskaya T P 1983 *Handbook of Glass Data, Part A: Silica Glass and Binary Silicate Glasses* (Amsterdam: Elsevier)

[23] Jund P and Jullien R 2000 *J. Chem. Phys.* **113** 2768
[24] Lekner J 1991 *Physica* A **176** 485
     Hautman J and Klein M L 1992 *Mol. Phys.* **75** 379
[25] Greengard L and Rokhlin V 1987 *J. Comput. Phys.* **73** 335
[26] de Leeuw S and Perram J 1979 *Mol. Phys.* **37** 1313
[27] Ahermouch M 1998 Fusion orientationnelle d'un cristal moléculaire, effets de surface. Simulation numérique
     de dynamique moléculaire *PhD Thesis* PA066376, Université Paris 6
[28] Allen M P and Tildesley D J 1990 *Computer Simulations of Liquids* (New York: Oxford University Press)
[29] Tse J S, Klug D D and Le Page Y 1992 *Phys. Rev.* B **46** 5933
[30] Chapela G, Saville G, Thompson S M and Rowlinson J S 1977 *J. Chem. Soc. Faraday Trans.* II **8** 133
[31] Iarlori S, Carnevali P, Ercolessi F and Tosatti E 1989 *Surf. Sci.* **211/212** 55
     Celestini F, Ercolessi F and Tosatti E 1997 *Phys. Rev. Lett.* **78** 3153
[32] Litton D A and Garofalini S H 1997 *J. Non Cryst. Solids* **217** 250
[33] Rino J, Ebbsjö I, Kalia R and Vashishta P 1993 *Phys. Rev.* B **47** 3053
[34] Dubois L H and Zegarski B R 1993 *J. Phys. Chem.* **97** 1665
[35] Bunker B C, Haaland D M, Ward K J, Michalske T A, Smith W L, Binkley J S, Melius C F and Balfe C A 1989
     Surf. Sci. **210** 406
[36] Morrow B A and Devi A 1972 *Trans. Faraday Soc.* **68** 403
     Morrow B A and Cody I A 1976 *J. Phys. Chem.* **80** 1995
[37] Lopez N, Vitiello M, Illas F and Pacchioni G 2000 *J. Non-Cryst. Solids* **271** 56
[38] See e.g. Tosatti E 1988 *The Structure of Surfaces II* ed J F van der Veen and M A Van Hove (Heidelberg:
     Springer) p 535
[39] Ballone P and Rubini S 1995 *Surf. Sci.* **342** L1116
     Jagla E A and Tosatti E 2000 *Surf. Sci.* **464** 1
[40] Beckers J V L and de Leeuw S W 2000 *J. Non-Cryst. Solids* **261** 87